Nathaniel T. Pickle
Department of Mechanical Engineering,
Colorado School of Mines,
1500 Illinois St,
Golden, CO 80401
e-mail: nathaniel.pickle@utdallas.edu

Alena M. Grabowski
Department of Integrative Physiology,
University of Colorado,
354 UCB,
Boulder, CO 80309;
VA Eastern Colorado Healthcare System,
Denver, CO 80220
e-mail: alena.grabowski@colorado.edu

Jana R. Jeffers
Department of Integrative Physiology,
University of Colorado,
354 UCB,
Boulder, CO 80309
e-mail: Jana.Jeffers@colorado.edu

Anne K. Silverman[1]
Department of Mechanical Engineering,
Colorado School of Mines,
1500 Illinois St,
Golden, CO 80401
e-mail: asilverm@mines.edu

The Functional Roles of Muscles, Passive Prostheses, and Powered Prostheses During Sloped Walking in People With a Transtibial Amputation

Sloped walking is challenging for individuals with transtibial amputation (TTA) due to the functional loss of the ankle plantarflexors. Prostheses that actively generate ankle power may help to restore this lost function. The purpose of this study was to use musculoskeletal modeling and simulation to quantify the mechanical power delivered to body segments by passive and powered prostheses and the remaining muscles in the amputated and intact legs during sloped walking. We generated walking simulations from experimental kinematic and kinetic data on slopes of 0, ±3 deg and ±6 deg in eight people with a TTA using powered and passive prostheses and eight nonamputees. Consistent with our hypothesis, the amputated leg hamstrings generated more power to both legs on uphill slopes in comparison with nonamputees, which may have implications for fatigue or overuse injuries. The amputated leg knee extensors delivered less power to the trunk on downhill slopes (effect size (ES) ≥ 1.35, $p \leq 0.02$), which may be due to muscle weakness or socket instability. The power delivered to the trunk from the powered and passive prostheses was not significantly different ($p > 0.05$), However, using the powered prosthesis on uphill slopes reduced the contributions from the amputated leg hamstrings in all segments (ES ≥ 0.46, $p \leq 0.003$), suggesting that added ankle power reduces the need for the hamstrings to compensate for lost ankle muscle function. Neither prosthesis replaced gastrocnemius function to absorb power from the trunk and deliver it to the leg on all slopes.
[DOI: 10.1115/1.4037938]

Introduction

People with a transtibial amputation (TTA) often have impaired mobility. For example, compared to nonamputees, people with a TTA using passive-elastic prostheses have greater joint kinematic and kinetic asymmetry [1–3], metabolic energy expenditure during level-ground walking [4–6], and prevalence of joint disorders and pain [7–9]. People with a TTA no longer have the function provided by the ankle plantarflexor muscles, including the uniarticular soleus and the biarticular gastrocnemius. These muscles are critical for performing the functional roles of providing forward propulsion, body support, and leg swing initiation during level-ground walking [10–13]. In this context, we define a "functional role" as the mechanical contributions from muscles and prostheses to whole-body movement. For example, during level-ground walking in nonamputees, both the soleus and gastrocnemius perform the functional roles of support (upward acceleration) and propulsion (forward acceleration) of the body center of mass (COM). The soleus performs this role by absorbing mechanical power from the leg and generating power to the trunk to accelerate the trunk forward. In contrast, the gastrocnemius absorbs power from the trunk and generates power to the leg for leg swing initiation [10].

In contrast to the soleus and gastrocnemius muscles, which perform net positive work during stance, passive-elastic prostheses perform net negative work over the stance phase [14]. Passive-elastic prostheses can partially replicate the function of the soleus in providing body support and delivering power to the trunk, but do not perform the function of the gastrocnemius in generating power to the ipsilateral leg during level-ground walking [12,14]. Powered ankle-foot prostheses, like the ankle plantarflexors, perform net positive work at the prosthetic ankle joint over the stance phase [15,16]. However, commercial powered prostheses do not actuate the knee joint like the biarticular gastrocnemius. In addition, powered prostheses are typically designed to produce local ankle joint mechanics that are similar to a biological ankle, such as matching biological ankle moment or work during walking. Reproducing local ankle joint mechanics has been successful in reducing the metabolic cost of level-ground walking compared to use of a passive-elastic prosthesis and normalizing metabolic cost compared to nonamputees [17]. However, the addition of prosthetic ankle power does not fully restore normative whole-body biomechanics, particularly during challenging tasks. These remaining deficits are evidenced by differences that persist in joint kinematics and kinetics on level ground [18], whole-body angular momentum during walking at various speeds [19] and on nonlevel surfaces [20,21], and proximal joint kinematics on uneven terrain [22]. How the addition of prosthetic ankle power affects the functional roles of lower-limb muscles during challenging walking tasks remains unclear. Quantifying prosthesis functional roles could aid in designing future prostheses to replicate the functional role of a biological ankle in contributing to whole-body movement rather than reproducing local ankle joint mechanics.

Walking on uphill and downhill slopes are important activities of daily living that can be challenging for many populations. For nonamputees, walking uphill requires an increased duration and magnitude of muscle activity in the hip extensors [23] and increased hip and ankle range of motion [24] compared to level-ground walking, while walking downhill requires increased duration and magnitude of knee extensor activity [23] and greater knee power absorption [25] compared to level-ground walking. Consistent with these observations, previous musculoskeletal

[1]Corresponding author.

Manuscript received May 15, 2017; final manuscript received September 15, 2017; published online October 10, 2017. Editor: Beth A. Winkelstein.

Table 1 Muscle group definitions and abbreviations. The muscles that we collected EMG data from are indicated by "E" and muscles in the group that were constrained based on the EMG signal are denoted by "C." EMG signals were not collected from the soleus, gastrocnemius or dorsiflexors in the amputated leg.

Group name	Muscles in group
Soleus	Soleus[EC]
Gastrocnemius	Lateral gastrocnemius[EC] Medial gastrocnemius[C]
Dorsiflexors	Tibialis anterior[EC] Extensor digitorum longus Extensor hallucis longus Peroneus tertius
Vasti	Vastus lateralis[EC] Vastus medialis[C] Vastus intermedius[C]
Rectus femoris	Rectus femoris[EC]
Hamstrings	Biceps femoris long head[EC] Gracilis Semimembranosus Semitendinosus
Gluteus maximus Hip abductors	Gluteus maximus (superior, middle, and inferior compartments)[EC] Gluteus medius (anterior, middle, and posterior compartments)[EC] Gluteus minimus (anterior, middle, and posterior compartments) Piriformis

modeling analyses of nonamputees have indicated that the hip extensors are important for generating power to both the swing and stance legs on inclines, and that the knee extensors absorb power from the ipsilateral leg during stance on declines [26]. Likewise, a predictive simulation of incline walking using a two-dimensional musculoskeletal model has demonstrated that increases in the peak and duration of force generated by the hamstrings and gluteus maximus during uphill walking were required as uphill angle increased [27]. In addition, prior musculoskeletal modeling studies have found that ankle, knee, and hip joint contact forces increase during uphill walking, and that hip and knee joint contact forces increase during downhill walking. The increases in joint compressive loads were attributed to higher forces from the hamstrings, vasti, gastrocnemius, and soleus during uphill walking and higher forces from the gluteus medius, rectus femoris, and vasti during downhill walking [28,29]. These prior studies highlight how muscle forces and power generation are adapted to achieve the altered demands of uphill and downhill walking compared to level-ground walking.

Uphill and downhill walking can be especially challenging for individuals with TTA. Specifically, one survey found that 85% of individuals with TTA reported some level of difficulty walking on slopes [30]. Furthermore, prior studies have shown compensations in other muscles, such as longer durations of muscle activity in the amputated leg hip extensors and intact leg knee extensors [31] and reduced contributions to body COM braking in the amputated leg knee extensors [12]. During uphill walking, individuals with TTA using both passive-elastic and powered prostheses rely on hip power generation more than nonamputees, as indicated by greater net hip joint power in the amputated leg [20]. During downhill walking, individuals with TTA using both passive-elastic and powered prostheses had reduced net knee joint power absorption in the amputated leg compared to nonamputees [32], possibly due to weakness of the quadriceps in the amputated leg [33] or discomfort due to socket pressure [34]. However, these prior studies of sloped walking in individuals with TTA reported joint-level moments and powers, but did not investigate the functional roles of individual muscles, which can only be achieved through a musculoskeletal modeling approach.

Thus, the goal of this study was to use musculoskeletal modeling and movement simulations to quantify the functional roles of passive-elastic and powered prostheses by investigating the amount of mechanical power each prosthesis delivered to the trunk and legs during sloped walking. Further, the functional roles of individual lower-limb muscles when using passive-elastic and powered prostheses were also investigated and compared with those of nonamputees. Based on the results of previous studies of net joint power [20,32], we hypothesized that individuals with TTA would use their hip extensors to generate more power to the legs compared to nonamputees on inclines and absorb less power from the ipsilateral leg with the knee extensors of the amputated leg compared to nonamputees on declines. We also hypothesized that both prostheses would absorb power from the leg and transfer it to the trunk, but that the powered prosthesis would generate more power to the trunk than the passive-elastic prosthesis. This increased trunk power generation was expected because the powered prosthesis actuates the ankle joint similarly to the uniarticular soleus muscle, which generates power to the trunk [10]. We expected that neither prosthesis would perform the function of the biarticular gastrocnemius to generate power to the leg because neither device actuates the knee joint.

Methods

Experimental Data Collection. Eight healthy adults (1 female and 7 males, 72 ± 8 kg, 177 ± 6 cm, 30 ± 8 years) and eight individuals with unilateral TTA (4 females and 4 males, 78 ± 12 kg, 172 ± 7 cm, 45 ± 11 years) provided written informed consent to participate in the experimental protocol approved by the Human Subjects Institutional Review Board at the Department of Veterans Affairs. Participants with TTA all underwent amputation due to trauma, self-reported as Medicare Functional Classification Level K3 or higher, and were free of neurological, cardiovascular, or musculoskeletal impairments other than that associated with the amputation. We matched participants with and without TTA based on height and weight. Participants stood in place for a static trial and then walked on an inclinable dual-belt force-measuring treadmill (Bertec Corp., Columbus, OH) at 1.25 m/s on slopes of 0 deg, ±3 deg, and ±6 deg while we simultaneously measured bilateral ground reaction forces (GRFs, 1500 Hz), whole-body kinematics (100 Hz, Vicon Inc., Centennial, CO), and electromyographic (EMG) signals (1500 Hz, Noraxon Corp., Scottsdale, AZ) from eight intact leg muscles and five amputated leg muscles (Table 1). Each trial was approximately 1 min long and we

collected data for 30 s. Reflective markers were placed bilaterally on joint centers, and clusters of at least four markers were placed on each body segment. We placed reflective markers at the approximate locations of the prosthetic foot corresponding to the first and fifth metatarsal heads, posterior calcaneus, and medial and lateral malleoli. Individuals with TTA performed the protocol using their clinically prescribed passive-elastic prosthesis as well as the BiOM (BiOM T2, BIONX Inc., Bedford, MA) powered prosthesis. Prior to experimental trials, we iteratively tuned the BiOM to match average biological ankle range of motion, peak moment, peak power, and net work at each slope [35]. Each participant walked using the BiOM prosthesis for 6–8 h over 3–4 days prior to data collection.

Musculoskeletal Model and Simulation Development. Kinematic marker trajectories were low-pass filtered with a 6 Hz cutoff frequency using a fourth-order bidirectional Butterworth filter in VISUAL3D (C-Motion, Inc., Germantown, MD). Joint angles were computed using a least squares optimization approach to inverse kinematics [36]. GRFs were also low-pass filtered with a 6 Hz cutoff to eliminate noise caused by vibrations in the treadmill [37–39] and maintain consistency between data types [40,41]. Musculoskeletal models of each participant were created in OpenSim 3.1 [42] by scaling the size and inertial properties of the body segments in a generic model [43,44] with 21 degrees-of-freedom (DOF) and 92 Hill-type musculotendon actuators with normative force-length-velocity properties [45]. The scale factors for each segment were computed in VISUAL3D from the static standing trial. Passive structures were represented by generalized torques applied to each rotational DOF as an exponential function of joint angle [46,47]. The prostheses were modeled by removing all muscles crossing the ankle joint in the musculoskeletal model, including the biarticular gastrocnemius, and replacing them with a generalized rotational actuator at the ankle. Thus, the mechanical properties of the devices, such as stiffness and damping, were not explicitly modeled, but the equivalent ankle moment provided by the passive and powered prostheses between the rigid foot and shank segments was computed using inverse dynamics. The subtalar joint of the prosthetic leg was locked. The inertial properties of the BiOM were assumed to be the same as a biological leg [17]. For the passive-elastic prosthesis, the distance between the knee joint and tibia COM was reduced by 25% [48] and the tibia mass was reduced by 50% [12]. During the simulations, residual forces and moments were applied to the pelvis in 6DOF to ensure dynamic consistency between the experimental and simulated motions. A residual reduction algorithm was used to minimize these residual forces and moments by adjusting the total model mass and torso COM location [42]. We then used a computed muscle control algorithm to determine muscle forces that reproduced the adjusted inverse kinematics solution from the residual reduction algorithm while minimizing the sum of squared muscle excitations. Simulated muscle excitations were constrained using processed EMG signals (Table 1). Raw EMG signals were processed by de-meaning, rectifying, and applying a bidirectional moving average filter with a window of 100 ms. For each trial, the processed EMG signal for each muscle was normalized by the peak signal value of that muscle across all trials for that person. Muscles in the simulation were constrained to have an excitation greater than 0.5 if the corresponding normalized EMG signal was greater than 0.5 for more than 0.01 s. Muscles in the simulation were constrained to have an excitation of less than 0.1 if the normalized EMG signal was less than 0.05 for more than 0.01 s. Otherwise, the muscle excitation bounds in the simulation were set at 0.02 and 1.0. Reserve torque actuators were applied at each joint to supplement the muscle forces if necessary.

We selected three gait cycles (i.e., three trials from heel strike to heel strike of the same leg) from each 30 s data collection in which all body segments were tracked and clean foot contacts were achieved on each belt of the treadmill. Walking simulations were then developed for the selected gait cycles at each of the five slopes for all participants and for both prostheses for participants with TTA. A total of 360 gait cycle simulations were generated.

Segment Power Analyses. We performed segment power analyses on the walking simulations to determine the instantaneous power delivered to the body segments by each force in the model [49]. We replaced the GRF with a "rolling without slipping" kinematic constraint [50] and solved the system equations of motion for the resulting accelerations due to each force acting on the model. The induced segment accelerations were multiplied by the segment velocities to calculate the power generated to (positive power) or absorbed from (negative power) each segment. The net power delivered to the trunk (pelvis and torso) and legs (toes, calcaneus, talus, tibia, and femur in each leg) was calculated by summing the linear and rotational power delivered to each body segment by each individual model force (e.g., muscle, prosthesis, gravity), and was then normalized by the total segment mass. Specifically, we investigated the power to the trunk and legs from a passive-elastic prosthesis, a powered prosthesis, and the following muscle groups (Table 1): hamstrings, gluteus maximus, rectus femoris, vasti, soleus, and gastrocnemius.

Statistical Comparisons. A linear mixed effects ANOVA [51] was used to compare the average power delivered to the trunk and legs by the muscles and prostheses during stance (0–60% of the respective leg gait cycle). A separate ANOVA was performed for each muscle group. Slope (0 deg, ±3 deg, and ±6 deg) and leg type (nonamputee leg, amputated leg using the powered prosthesis, intact leg using the powered prosthesis, amputated leg using a passive-elastic prosthesis, and intact leg using a passive-elastic prosthesis) were fixed effects in the model and participant was a random intercept effect. When a significant main or interaction effect was found, post hoc comparisons were performed using least squares means [52]. Tukey's method was used to maintain a critical threshold of $p = 0.05$ for each family of comparisons. We reported the standardized effect size (ES) as the magnitude of difference in estimated means divided by the standard deviation of the residuals in the linear mixed effects model. In general, an ES of 0.2 or less is "small," between 0.2 and 0.8 is "medium," and greater than 0.8 is "large." We also reported the magnitude of the upper and lower 95% confidence intervals (CIs) for the differences in estimated means. The CI values are reported in W/kg.

Results

The largest root-mean-squared (RMS) rotational kinematic errors in the simulations occurred in the prosthetic ankle (1.55 ± 0.99 deg, average and standard deviation across participants with TTA) and lumbar extension (1.88 ± 1.00 deg, average and standard deviation across nonamputees), and the largest RMS translational errors were 1.95 ± 1.02 cm in pelvis mediolateral translation in participants with TTA and 1.83 ± 0.21 cm in pelvis anterior/posterior translation in nonamputees (Table 2). The greatest mean RMS residual force was 1.60 ± 0.79% body weight (BW) in the vertical direction at +6 deg and the greatest mean RMS residual moment was 2.32 ± 1.21%BW m about the anterior axis, which both occurred in the TTA simulations (Table 3). Simulated muscle excitation profiles were similar to the processed EMG signals for both individuals with TTA (Fig. 1) and nonamputees (Fig. 2), though the vasti and rectus femoris excitation in the amputee simulations had smaller magnitudes than the experimental EMG signals (Fig. 1).

Hip Extensors. There were significant main effects in the power generated to the trunk and both legs by the hamstrings, but no significant interaction effects. There were significant main and interaction effects in the power generated to the trunk and ipsilateral leg by the gluteus maximus, but only the main effects

Table 2 Mean (standard deviation) RMS tracking errors for each DOF in the model, along with mean (standard deviation) RMS reserve actuator moments. Results of participants with TTA are averaged across all passive and powered prosthesis simulations. Tracking errors are in units of degrees except for pelvis anterior, vertical, and mediolateral position, which are in centimeters. The reserve actuator moments are normalized by each person's body mass (Nm/kg). The prosthetic subtalar joint is not applicable (N/A) because that joint was locked during simulation.

	Error		Reserves (Nm/kg)	
	TTA	Nonamputee	TTA	Nonamputee
Lumbar extension	1.42 (0.85)	1.55 (0.99)	0.001 (0.02)	0.001 (0.01)
Lumbar bending	0.93 (0.50)	0.87 (0.52)	0.001 (0.01)	0.000 (0.00)
Lumbar rotation	0.74 (0.60)	0.62 (0.55)	0.000 (0.00)	0.000 (0.00)
Amputated/right hip flexion	0.62 (0.38)	0.72 (0.61)	0.037 (0.06)	0.009 (0.01)
Amputated/right hip adduction	0.63 (0.45)	0.58 (0.54)	0.038 (0.07)	0.012 (0.01)
Amputated/right hip rotation	0.25 (0.17)	0.28 (0.38)	0.014 (0.02)	0.010 (0.01)
Amputated/right knee flexion	0.75 (0.37)	0.39 (0.30)	0.063 (0.12)	0.028 (0.03)
Amputated/right ankle flexion	1.83 (0.21)	1.36 (2.29)	0.539 (0.11)	0.087 (0.05)
Amputated/right subtalar inversion	N/A	0.40 (0.39)	N/A	0.017 (0.01)
Intact/left hip flexion	0.73 (0.43)	0.60 (0.47)	0.013 (0.02)	0.008 (0.02)
Intact/left hip adduction	0.66 (0.50)	0.50 (0.59)	0.020 (0.04)	0.012 (0.02)
Intact/left hip rotation	0.25 (0.18)	0.23 (0.15)	0.012 (0.03)	0.006 (0.01)
Intact/left knee flexion	0.40 (0.26)	0.41 (0.33)	0.030 (0.03)	0.014 (0.03)
Intact/left ankle flexion	0.34 (0.25)	0.43 (0.34)	0.077 (0.05)	0.040 (0.03)
Intact/left subtalar inversion	0.39 (0.22)	0.47 (0.68)	0.015 (0.01)	0.010 (0.01)
Pelvis tilt	0.14 (0.09)	0.17 (0.27)		
Pelvis list	0.17 (0.11)	0.20 (0.36)		
Pelvis rotation	0.23 (0.18)	0.16 (0.12)		
Pelvis anterior	1.89 (1.07)	1.88 (1.00)		
Pelvis vertical	1.94 (0.95)	1.78 (0.86)		
Pelvis mediolateral	1.95 (1.02)	1.67 (0.97)		

Table 3 Mean (standard deviation) RMS residual forces and moments applied to the pelvis to maintain dynamic consistency in the simulations. Results of participants with TTA are averaged across all passive and powered prosthesis simulations. Values were normalized to a percentage of body weight (%BW).

		Forces (%BW)			Moments (%BW-m)		
	Slope	A/P	Vertical	M/L	Frontal	Transverse	Sagittal
TTA	6	1.09 (1.20)	1.60 (0.79)	1.25 (1.34)	2.32 (1.21)	1.10 (0.50)	2.50 (1.20)
	3	0.92 (0.50)	1.32 (0.65)	0.91 (0.97)	1.94 (0.93)	0.94 (0.52)	2.13 (0.71)
	0	0.90 (0.47)	1.26 (0.43)	0.83 (0.79)	1.50 (0.47)	0.85 (0.39)	1.80 (0.52)
	−3	1.04 (0.58)	1.33 (0.44)	0.72 (0.49)	1.68 (0.82)	0.96 (0.50)	1.86 (0.55)
	−6	0.92 (0.41)	1.35 (0.43)	0.62 (0.28)	1.74 (0.75)	0.97 (0.36)	1.91 (0.59)
Nonamputee	6	0.86 (0.61)	1.42 (0.65)	0.79 (0.39)	1.64 (0.58)	0.72 (0.15)	2.13 (0.54)
	3	0.58 (0.31)	0.75 (0.31)	0.63 (0.44)	1.59 (0.84)	0.81 (0.15)	1.65 (0.29)
	0	0.94 (0.82)	0.70 (0.57)	0.75 (0.53)	1.46 (0.52)	0.85 (0.16)	1.76 (0.65)
	−3	0.52 (0.41)	1.11 (0.99)	0.66 (0.40)	1.30 (0.41)	0.92 (0.17)	1.69 (0.65)
	−6	0.59 (0.40)	1.07 (1.12)	0.65 (0.40)	1.32 (0.43)	0.96 (0.16)	1.58 (0.60)

were significant for the power delivered to the contralateral leg (Table 4). The amputated leg hamstrings absorbed more power from the trunk and generated more power to both legs than the intact leg hamstrings when using both passive-elastic and powered prostheses on all slopes (Fig. 3, all $p < 0.001$). The average trunk power absorption from the amputated leg hamstrings compared to the intact leg hamstrings was greater by 0.74 W/kg on average ($p < 0.001$, ES = 0.96, CI = [0.47,1.01]) when using a passive-elastic prosthesis and greater by 0.64 W/kg on average ($p < 0.001$, ES = 0.84, CI = [0.37,0.91]) when using a powered prosthesis (Fig. 3). When using a passive-elastic prosthesis, the amputated leg hamstrings generated 110% more power to the ipsilateral leg compared to nonamputees ($p < 0.001$, ES = 1.60, CI = [1.44,4.21]) and also generated 92% more power to the contralateral leg compared to nonamputees ($p < 0.001$, ES = 1.25, CI = [0.87,3.57]) on average across all slopes. There were no differences in the power absorbed from the trunk or generated to the ipsilateral leg by the hamstrings when using a powered prosthesis compared to nonamputees. However, the power generated to the contralateral leg by the amputated leg hamstrings when using a powered prosthesis was on average 56% greater ($p = 0.04$, ES = 0.78, CI = [0.04,2.74]) compared to nonamputees across all slopes. In addition, the amputated leg hamstrings absorbed significantly less power from the trunk ($p < 0.001$, ES = 0.53, CI = [0.13,0.67]) and generated more power to the ipsilateral leg ($p < 0.001$, ES = 0.96, CI = [1.07,2.31]) and contralateral leg ($p = 0.003$, ES = 0.46, CI = [0.20,1.45]) when using a powered compared to a passive-elastic prosthesis. This difference when using passive and powered prostheses occurred during approximately 20–50% of the prosthetic leg gait cycle (Fig. 4) The amount of power generated to the contralateral leg by the gluteus maximus was significantly different between the amputated and intact legs when using both the passive ($p < 0.001$, ES = 1.00, CI = [0.26,0.55]) and powered ($p < 0.001$, ES = 0.42, CI = [0.03,0.32]) prostheses at all slopes and was significantly greater in the intact leg when using a passive-elastic prosthesis compared to nonamputees on all slopes ($p = 0.04$, ES = 0.92, CI = [0.01,0.74]).

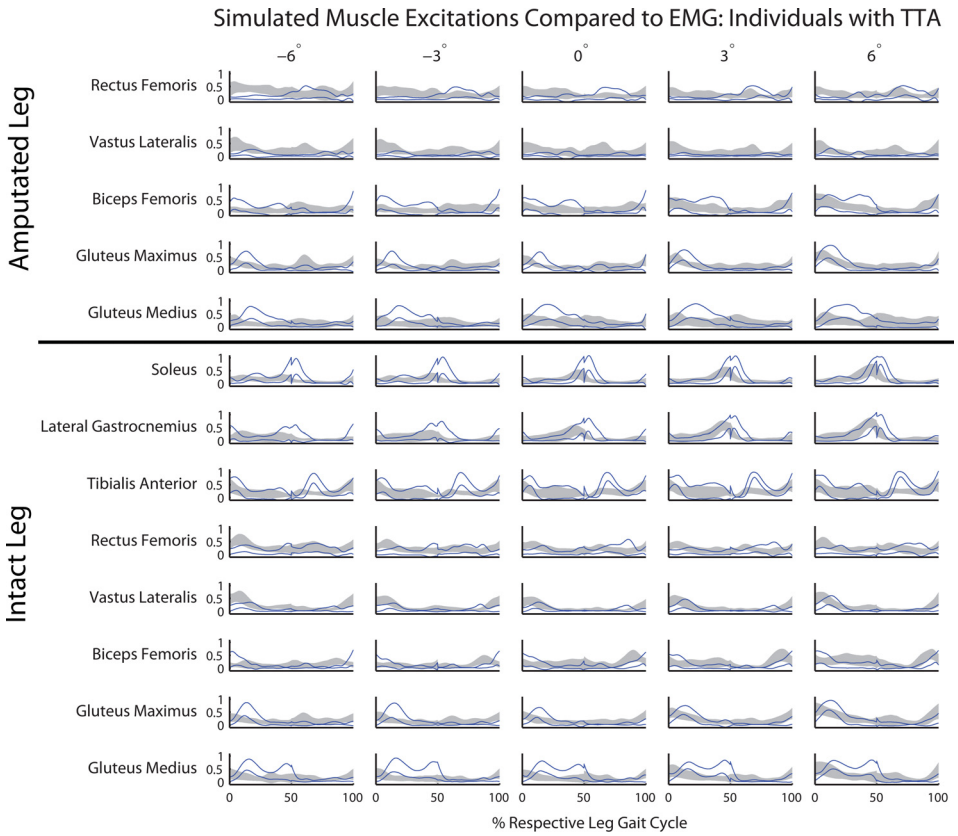

Fig. 1 Comparison of the mean (±standard deviation) processed EMG signals from each muscle group (shaded area) and the mean (±standard deviation) of the processed muscle excitations in the simulations for individuals with TTA using both prostheses (upper and lower bounds indicated by solid lines). Discontinuities in the simulation traces are a result of the gait cycle normalization we used for visualization purposes to be consistent across people with left and right leg amputations. The discontinuities reflect the end points of full gait cycle simulations and do not affect the results.

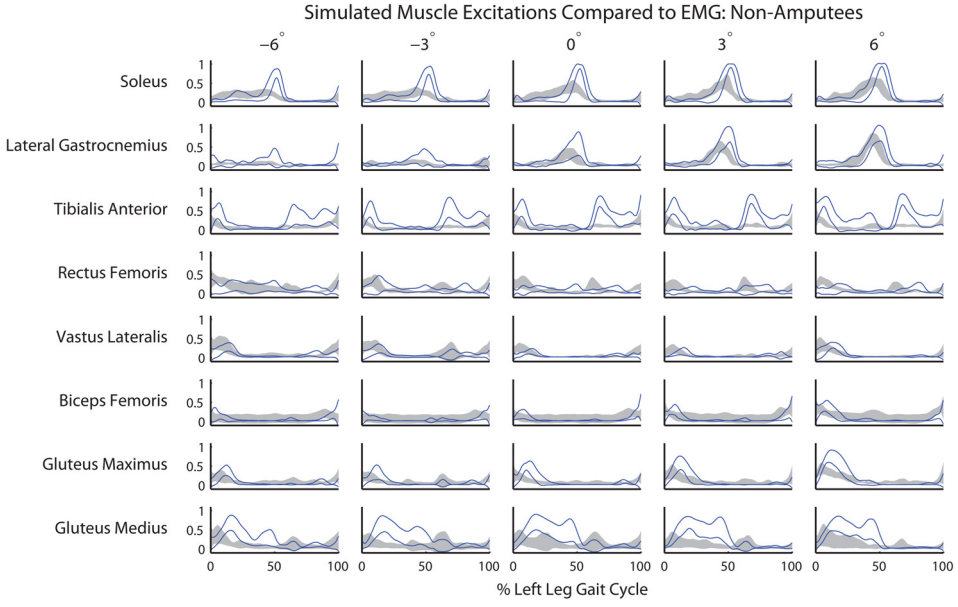

Fig. 2 Comparison of the mean (±standard deviation) processed EMG signals from each muscle group (shaded area) and the mean (±standard deviation) of the processed muscle excitations in the simulations for nonamputees (upper and lower bounds indicated by solid lines)

Table 4 Statistical results of significant main and interaction effect *p*-values from the ANOVA. Values of "0" indicate that the *p*-value was less than 0.001. *p*-values for the contralateral leg are not reported (N/R) because these comparisons were not relevant to the hypotheses. "—" indicates the result was not significant.

	Trunk			Ipsilateral leg			Contralateral leg		
	Slope	Leg	Interaction	Slope	Leg	Interaction	Slope	Leg	Interaction
Ankle sum/prosthesis	0	0	0	0	0	0		N/R	
Soleus	0	0	0	0	0	0			
Gastrocnemius	0	0	0	0	0	0			
Rectus femoris	0	0	0	0	0	0		N/R	
Vasti	0	0.004	0	0	—	0			
Hamstrings	0	0	—	0	0	—	0	0	—
Gluteus maximus	0	0	0	0	0	0	0	0	—

Knee Extensors. The main and interaction effects were significant for the rectus femoris and vasti in the power delivered to the trunk and ipsilateral leg, with the exception of the main effect of leg in the power delivered to the ipsilateral leg by the vasti, which was not significant (Table 4). The rectus femoris in the amputated leg generated an average of 49% less power to the trunk in comparison with the intact leg on all slopes when using a passive-elastic prosthesis (Fig. 5, all $p \leq 0.004$ and ES ≥ 1.25). In addition, at −6 deg and −3 deg the power generated to the trunk by the amputated leg rectus femoris was reduced compared to nonamputees with both the passive-elastic (−6 deg: $p < 0.001$, ES = 1.71, CI = [0.20,1.35]; −3 deg: $p = 0.021$, ES = 1.35, CI = [0.04,1.18]) and powered (−6 deg: $p = 0.013$, ES = 1.39, CI = [0.06,1.20]; −3 deg: $p = 0.011$, ES = 1.41, CI = [0.07,1.21]) prostheses. At +3 deg and +6 deg the power generated to the trunk by the intact leg rectus femoris was increased compared to nonamputees with the passive-elastic prosthesis (+3 deg: $p < 0.001$, ES = 1.66, CI = [0.18,1.32]; +6 deg: $p = 0.01$, ES = 1.42, CI = [0.07,1.21]). There were relatively few differences in vasti function between conditions, with the only strong significant difference ($p < 0.001$, ES = 1.45, CI = [0.07,0.47]) occurring in the amount of power delivered to the trunk by the intact compared to amputated leg at +6 deg when using the passive-elastic prosthesis.

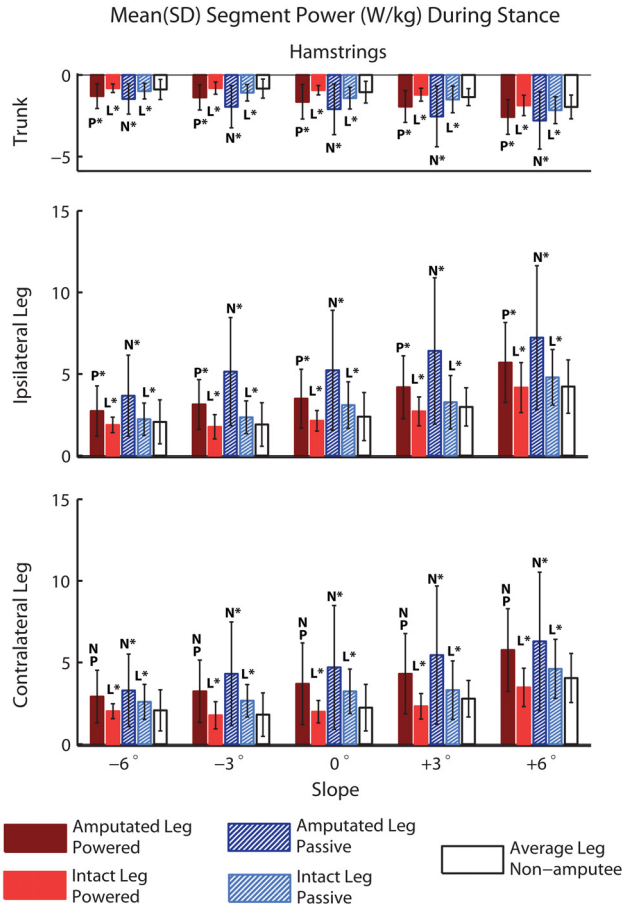

Fig. 3 Mean (±standard deviation across all trials) power delivered to the trunk, ipsilateral leg, and contralateral leg by the hamstrings in the intact, amputated, and average nonamputee leg during stance at slopes of 0 deg, ±3 deg, and ±6 deg. Values are normalized by segment mass. Significant differences are indicated between intact and amputated leg (L), passive-elastic and powered prostheses (P), and compared to nonamputees (N), with *p*-values <0.001 indicated by "*." Individuals with TTA relied more heavily on the hamstrings compared to nonamputees, but use of a powered prosthesis reduced this hamstring compensation compared to use of a passive-elastic prosthesis.

Prosthesis and Ankle Muscles. All main and interaction effects were significant in the power delivered to the trunk and ipsilateral leg by both prostheses, summed ankle muscles (i.e., all uniarticular and biarticular muscles crossing the ankle joint), soleus, and gastrocnemius (Table 4). The amount of power delivered to the trunk was significantly different between the prosthesis and net intact ankle muscles when using both prostheses on all slopes (all $p < 0.001$, ES ≥ 1.45). At −6 deg, both prostheses absorbed approximately half as much power from the trunk as the intact ankle. At +6 deg, the passive-elastic and powered prostheses delivered 0.64 ± 0.62 and 0.56 ± 0.48 W/kg of positive power to the trunk, respectively, while the intact ankle generated 0.04 ± 0.59 W/kg to the trunk when using the passive-elastic prosthesis and absorbed -0.07 ± 0.55 W/kg when using the powered prosthesis (Fig. 6). Both the passive-elastic and powered prostheses absorbed significantly less power from the trunk than the sum of the nonamputee ankle muscles on level ground and inclines (Figs. 6 and 7), with $p < 0.001$ and ES ≥ 3.00 in all cases except for the powered prosthesis at 0 deg ($p = 0.01$, ES = 2.16, CI = [0.06,1.23]) and +3 deg ($p = 0.03$, ES = 2.02, CI = [0.02,1.19]), which were still statistically significant. The passive-elastic prosthesis absorbed power from the ipsilateral leg on level ground and uphill slopes, which was different from the power generated to the ipsilateral leg by the nonamputee ankle muscles (all $p < 0.001$, ES ≥ 2.36). The powered prosthesis absorbed less power from the ipsilateral leg compared to the passive-elastic prosthesis at 0 deg ($p < 0.001$, ES = 1.43, CI = [0.57,3.79]) and +3 deg ($p < 0.001$, ES = 1.66, CI = [0.92, 4.15]), but at +6 deg the powered prosthesis also absorbed more power from the ipsilateral leg in comparison with the nonamputee ankle muscles ($p < 0.001$, ES = 2.29, CI = [0.90,6.09]). In general, there was large variability across all participants with TTA in the amount of power delivered to the body segments by both the passive-elastic and powered prostheses (Fig. 6). For example, the

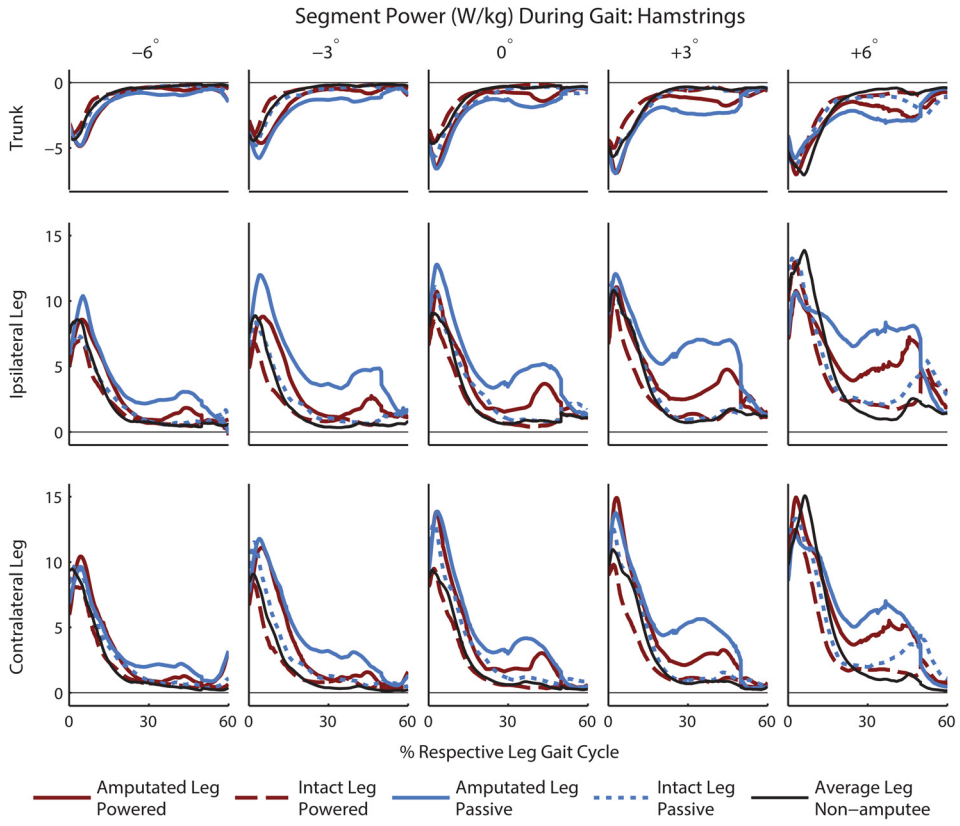

Fig. 4 Average power delivered to the trunk, ipsilateral leg, and contralateral leg by the hamstrings muscles in the intact, amputated and average nonamputee leg during stance (0–60% gait cycle) at slopes of 0 deg, ±3 deg, and ±6 deg. Values are normalized by segment mass. Use of a powered prosthesis reduced hamstrings compensations in the amputated leg compared to using a passive prosthesis, primarily during midstance (approximately 20–50% prosthetic leg gait cycle).

power delivered to the ipsilateral leg had a standard deviation across all subjects of between 3.1 and 3.6 W/kg with the passive prosthesis and 1.9 and 2.6 W/kg with the powered prosthesis, while the standard deviation from the nonamputee ankle was between 0.9 and 1.3 W/kg.

Discussion

In this study, we generated simulations of eight individuals with TTA and eight nonamputee individuals walking on 0 deg, ±3 deg, and ±6 deg slopes in order to investigate muscle and prosthesis functional roles. We expected that, compared to nonamputees, individuals with TTA would use the hip extensor muscles to generate more power to the legs on inclines and that their amputated leg knee extensors would absorb less power from the ipsilateral leg on declines. We also expected that the passive-elastic prosthesis would generate less power to the trunk compared to either the powered prosthesis or nonamputees. Neither prosthesis was expected to generate power to the leg in late stance like the nonamputee biarticular gastrocnemius.

Our first hypothesis regarding hip extensor function on inclines was supported. Individuals with TTA used a hip compensation strategy during uphill walking regardless of prosthetic foot type. The hamstrings in the amputated leg absorbed more power from the trunk and generated more power to both legs on nearly all slopes compared to the intact leg, suggesting that individuals with TTA rely heavily on the amputated leg hamstrings during uphill walking. Our results of greater power delivery from the hamstrings are consistent with prior work that found greater net hip joint power in the amputated leg during uphill walking on overground slopes of +5 deg and +10 deg at 1.28 ± 0.11 m/s with passive and powered prostheses [20] and at approximately +7 deg at 1.14 m/s with passive prostheses [33]. However, our simulations add to this prior work by demonstrating that individuals with TTA relied more on the biarticular hamstrings than on the uniarticular gluteus maximus to absorb power from the trunk and generate power to the ipsilateral leg. These findings are similar to previous level-ground simulation studies that showed that the hamstrings are the key muscle group used to compensate for the low stiffness of a passive-elastic prosthesis [31]. However, we also found that using a powered prosthesis reduced hamstring compensations during uphill walking, largely during midstance (approximately 20–50% prosthetic leg gait cycle, Fig. 4). These findings may have implications for individuals with TTA who also have hamstrings weakness or injury. These individuals may be unable to navigate sloped surfaces due to the demand placed on the hamstrings, but use of a powered prosthesis may assist these individuals. The results of the hamstrings also highlight that the addition of prosthetic ankle joint power affects the functional roles of other muscles in the body, and the effects of different prostheses on the entire musculoskeletal system should be considered during device prescription and in future design. Notably, a prior study that examined net hip joint power found significantly greater net hip extensor power in people with TTA compared to nonamputees on inclines, regardless of whether a powered or passive prosthesis was used [20]. However, in this prior study the powered prosthesis was tuned to match generic biological ankle mechanics only during level-ground walking. In contrast, in the present study the powered prosthesis was tuned to reproduce nonamputee ankle joint mechanics at each slope. These results

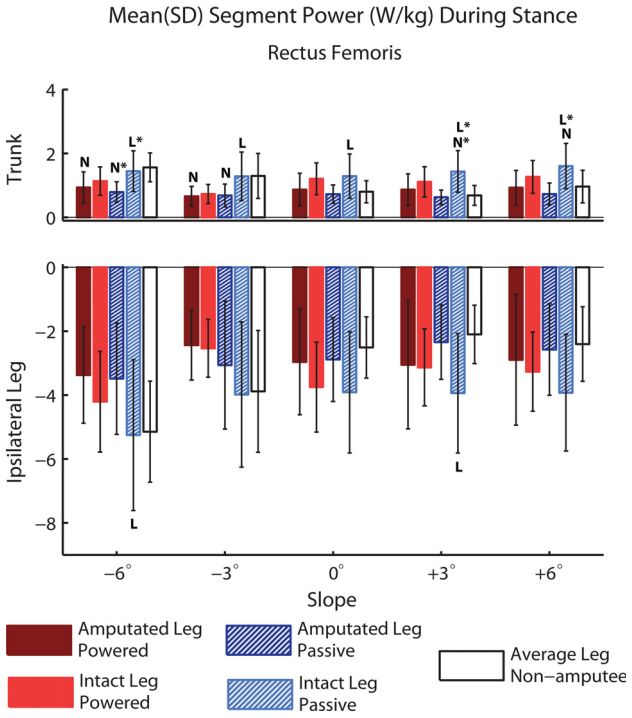

Fig. 5 Mean (± standard deviation across all trials) power delivered to the trunk and ipsilateral leg by the rectus femoris in the intact, amputated, and nonamputee leg during stance at slopes of 0 deg, ±3 deg, and ±6 deg. Significant differences are indicated between intact and amputated leg (L), passive and powered prosthesis (P), and compared to nonamputees (N), with *p*-values <0.001 indicated by "*." Values are normalized by segment mass. The amputated leg rectus femoris transferred less power from the leg to the trunk at −6 deg compared to nonamputees.

suggest that specific tuning of the powered prosthesis for different walking conditions may be helpful for taking full advantage of additional ankle power.

Our hypothesis regarding reduced knee extensor function in the amputated leg to absorb power from the leg and transfer it to the trunk on declines was also supported. The rectus femoris in the amputated leg delivered less power to the trunk and absorbed less power from the ipsilateral leg compared to the intact leg rectus femoris when walking at −6 deg (Fig. 5). Both the passive-elastic and powered prostheses absorbed less power from the trunk when walking at −6 deg (Fig. 6), which may suggest a decreased need for power delivery to the trunk from the rectus femoris. This result is similar to previous level-ground simulation results, which found that the rectus femoris in the amputated leg contributes less to braking of the body COM compared to nonamputees [12], and may be related to atrophy of the knee extensors that can occur in individuals with TTA [53]. The simulated rectus femoris and vasti excitations were lower in magnitude than the observed EMG in those muscles of individuals with TTA (Fig. 1), which may exaggerate the reductions in power absorbed in the simulations. However, we did not alter muscle strengths in our musculoskeletal models of participants with TTA, and people with TTA often have atrophy of the amputated leg quadriceps muscles [54]. Given the nominal muscle strength used in the model, this reduced muscle excitation is likely indicative of the reduced force from, and potentially reduced muscle strength of, the knee extensors to achieve the observed walking kinematics. Prior studies have also observed a decrease in knee flexion (i.e., a more extended knee) in the amputated leg during early and mid-stance of downhill walking compared to the intact leg [32]. While knee angle in the amputated leg was highly variable among participants in the present study (Fig. 8), several participants had decreased knee flexion during downhill walking compared to nonamputees. This strategy may reduce demands on the knee extensor muscles, and may also be related to socket fit. Poor socket fit or restrictions in movement imposed by the socket may lead to the sensation of instability at the interface between the socket and residual limb, which people with a TTA may counteract by extending their knee in order to transmit more of the load axially and reduce the knee flexion moment. These specific factors that may influence the reduction of knee extensor function should be further investigated.

Our hypothesis that use of a powered prosthesis would deliver more power to the trunk compared to the use of a passive-elastic prosthesis was not supported. In fact, the only significant difference between prostheses was that the powered prosthesis generated less power to the trunk compared to the passive-elastic prosthesis at +3 deg (Fig. 6). This result was surprising given that the soleus generates power to the trunk [10], and we expected the powered prosthesis to perform this function to a greater extent than a passive prosthesis. However, despite the lack of direct differences in function between prostheses, the powered prosthesis reduced the compensation in the amputated leg hamstrings (Fig. 3). There are several possible explanations for the lack of differences between prostheses, even though the powered prosthesis performs net positive work during the stance phase. First, neither prosthesis performed the function of the biarticular gastrocnemius, which transferred power from the trunk to the leg on all slopes (Fig. 6). Particularly on inclines, the gastrocnemius dominated the net power absorbed from the trunk during mid to late stance (Fig. 7, top row). Notably, the powered prosthesis did not simply exaggerate the functional role of the passive-elastic prosthesis (i.e., increased extrema), but rather functioned more similarly to the nonamputee soleus; absorbing less power from the leg than the passive-elastic prosthesis during approximately 30–50% of the gait cycle and delivering more power to the trunk during approximately 50–60% of the gait cycle (Fig. 7). While these results should be interpreted with caution due to the large variability in the amount of power delivered to the trunk and leg from both prostheses (Fig. 6), our findings suggest that use of the powered prosthesis reduces demand on the musculoskeletal system in comparison with use of a passive prosthesis.

The results of this study should be interpreted in the context of the limitations. Estimates of muscle forces from a simulation can be sensitive to the cost function and optimization framework [55,56] as well as to modeled muscle parameters, such as maximum isometric force [57]. Muscle parameters are difficult to measure but can differ between individuals of different ages or sex, and can also be affected by weakness in the amputated leg. As the participant groups in our study had different age (45 ± 11 and 30 ± 8) and sex (7M/1F and 4M/4F) distributions and we did not model amputated leg muscle weakness, a future sensitivity study would be useful to quantify the effects of these uncertainties on our results. However, we chose subjects of similar height and weight in order to make the physical characteristics of each group as similar as possible. In addition, muscle functional roles to accelerate and decelerate body segments can be sensitive to how ground contact is modeled [58]. However, we used the same simulation framework, cost function, and ground contact model for simulations of all participants, and thus the effects of these assumptions are consistent across all slope and leg conditions. In modeling participants with TTA, we approximated the behavior of the prostheses using a single torque actuator at the ankle joint. Our modeling approach is similar to that often used in inverse dynamics analyses of both nonamputees and individuals with TTA, which assume rigid prosthetic and biological feet, but may have an effect on our segment power calculations. Further, we assumed the interface between the residual limb and prosthetic socket to be rigid. Accurately measuring and simulating the socket/limb interface through nonrigid interface mechanics should be investigated in future work. The participants in our study were

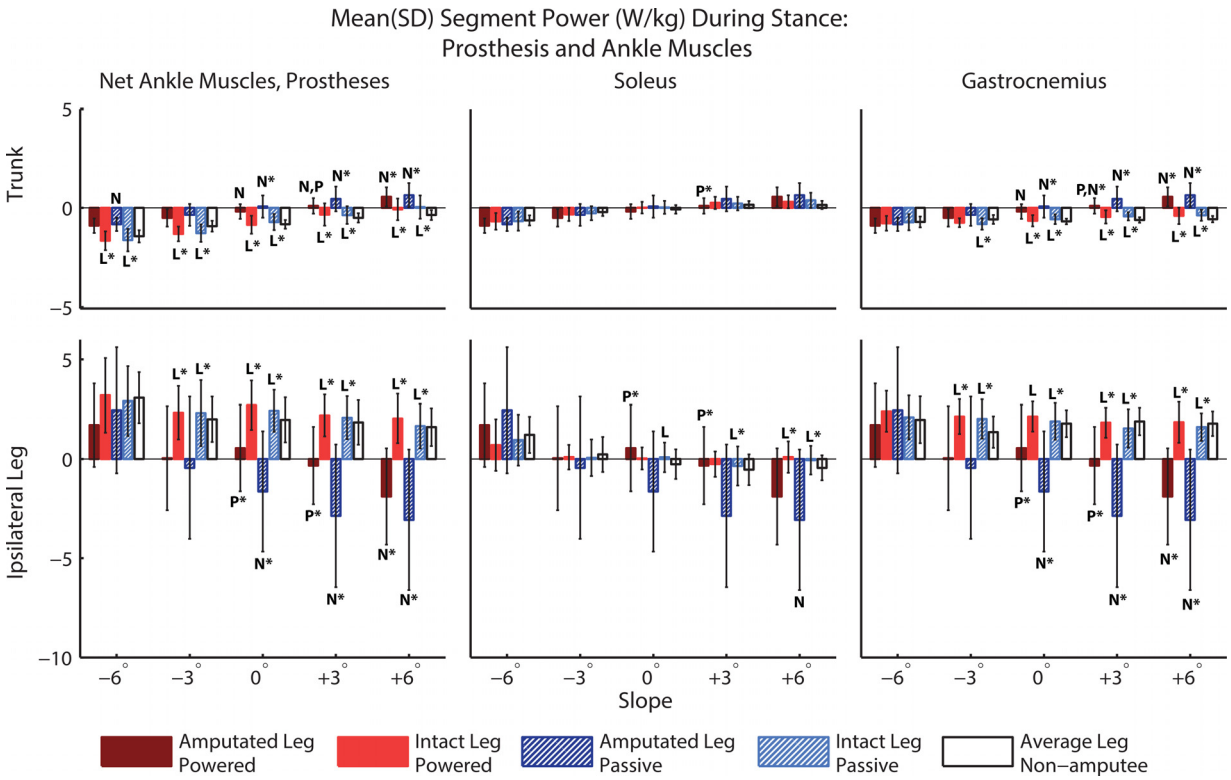

Fig. 6 The left column gives the mean (±standard deviation across all trials) power delivered to the trunk and ipsilateral leg by the passive and powered prostheses compared to the summed contributions of all ankle muscles in the intact and nonamputee legs. Thus, these plots compare the functional roles of each prosthesis and the biological ankle. The middle and right columns compare the passive and powered prostheses (same values as in left column) to the soleus and gastrocnemius of the intact and nonamputee legs. Values are normalized by segment mass. Significant differences are indicated between intact and amputated leg (L), passive, and powered prosthesis (P) and compared to nonamputees (N), with *p*-values <0.001 indicated by "*."

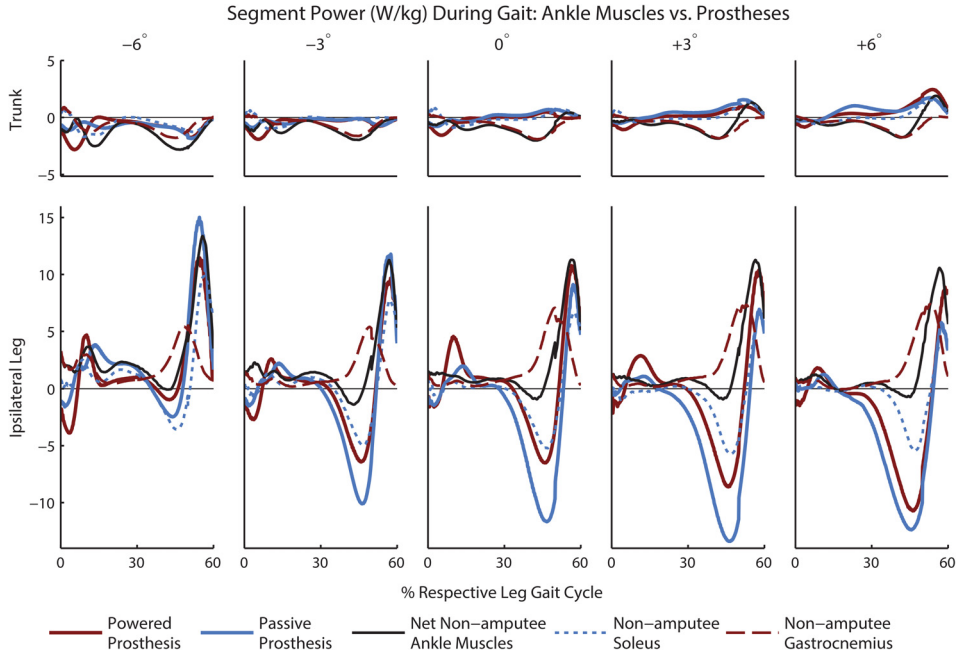

Fig. 7 Average power delivered to the trunk, ipsilateral leg, and contralateral leg by the powered and passive prostheses compared to the soleus, gastrocnemius, and sum of all ankle muscles in the nonamputee leg during stance (0–60% gait cycle) at slopes of 0 deg, ±3 deg, and ±6 deg. Values are normalized by segment mass.

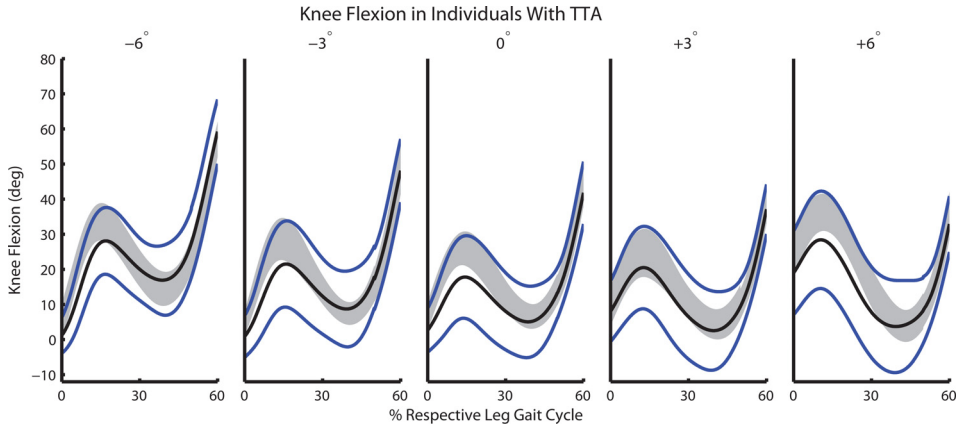

Fig. 8 Mean (±standard deviation) knee flexion angle during stance for nonamputees (shaded area) and the amputated leg of individuals with TTA using both prostheses (lines indicate mean and upper and lower bounds of one standard deviation). There was large variation in knee angle across participants with an amputation, which may partially explain the large variability in segment power generated by the muscles of the amputated leg.

given multiple days to adapt to using the powered prosthesis, but additional adaptation time may improve user performance. Finally, our study analyzed three trials per condition for eight participants in each group, which is small from a statistical perspective. Nonetheless, the large effect sizes (many >0.8) of our key findings give us confidence in these results.

Our results provide important information for future powered prosthesis control algorithm design. For example, an alternative to tuning prosthetic power delivery to match average nonamputee ankle mechanics is to design the timing and magnitude of power delivery to replicate functional roles of the biological ankle muscles. Altered timing and power magnitude of the powered prosthesis may potentially result in greater differences between prostheses in distributing power between the trunk and legs and fewer differences between people with and without TTA. Also, the current results are based on simulations generated to match experimental data. Other studies have used a predictive approach in which prosthesis characteristics can be altered in silico [14,31]. Our results provide a basis for future predictive simulation studies involving novel control of powered prostheses, with the goal of minimizing compensations in other muscles, such as the hamstrings and rectus femoris. A prosthesis that restores the functional roles normally performed by the biological ankle muscles may in turn improve mobility and reduce comorbidities such as joint pain for people with leg amputation.

Conclusion

We generated musculoskeletal simulations of individuals with and without transtibial amputations walking on inclines and declines. We identified hip muscle compensations from the hamstrings, but not the gluteus maximus, in the amputated leg. The hamstrings in the amputated leg absorbed more power from the trunk and generated more power to the legs compared to the intact leg and nonamputees. During walking at −6 deg, the rectus femoris in the amputated leg for both prostheses generated less power to the trunk and absorbed less power from the ipsilateral leg compared to the intact leg and nonamputees, consistent with other studies that have shown reduced braking of the body COM from the knee extensors of the amputated leg. There were few differences between the passive-elastic and powered prostheses in the average power delivered to the trunk and legs during stance, although use of the powered prosthesis reduced the compensations in the amputated leg hamstrings compared to use of the passive-elastic prosthesis. Consistent with other simulation studies of level-ground walking, both the passive-elastic and powered prostheses absorbed power from the leg and delivered it to the trunk during stance, which is similar to the function of the uniarticular soleus and dissimilar to the function of the biarticular gastrocnemius. The results of this study suggest that use of a powered prosthesis provides functional benefits compared to use of a passive-elastic prosthesis by reducing the hamstrings compensation strategy, but that neither prosthesis provides the function of the gastrocnemius for a wide range of slopes.

Acknowledgment

This work was supported by the Eunice Kennedy Shriver National Institute of Child Health & Human Development of the National Institutes of Health under Award Number R03HD075946 and a Career Development Award #A7972-W from the United States (U.S.) Department of Veterans Affairs Rehabilitation Research and Development Service. The content is solely the responsibility of the authors and does not necessarily represent the official views of the National Institutes of Health. Also, the contents do not represent the views of the U.S. Department of Veterans Affairs or the United States Government. NCT01784003.

Funding Data

- National Institute of Child Health and Human Development (Award No. R03HD075946).
- U.S. Department of Veterans Affairs (Award No. A7972-W).

Nomenclature

CI = confidence interval
COM = center of mass
DOF = degrees-of-freedom
EMG = electromyography
ES = effect size
GRF = ground reaction force
TTA = transtibial amputation

References

[1] Winter, D. A., and Sienko, S. E., 1988, "Biomechanics of Below-Knee Amputee Gait," J. Biomech., **21**(5), pp. 361–367.
[2] Sanderson, D., and Martin, P., 1997, "Lower Extremity Kinematic and Kinetic Adaptations in Unilateral Below-Knee Amputees During Walking," Gait Posture, **6**(2), pp. 126–136.
[3] Silverman, A. K., Fey, N. P., Portillo, A., Walden, J. G., Bosker, G., and Neptune, R. R., 2008, "Compensatory Mechanisms in Below-Knee Amputee

Gait in Response to Increasing Steady-State Walking Speeds," Gait Posture, **28**(4), pp. 602–609.
[4] Waters, R., Perry, J., and Antonelli, D., 1976, "Energy Cost of Walking of Amputees: The Influence of Level of Amputation," J. Bone Jt. Surg. Am., **58**(1), pp. 42–46.
[5] Hunter, D., Cole, E. S., Murray, J. M., and Murray, T. D., 1995, "Energy Expenditure of Below-Knee Amputees During Harness-Supported Treadmill Ambulation," J. Orthop. Sports Phys. Ther., **21**(5), pp. 268–276.
[6] Hsu, M.-J., Nielsen, D. H., Lin-Chan, S.-J., and Shurr, D., 2006, "The Effects of Prosthetic Foot Design on Physiologic Measurements, Self-Selected Walking Velocity, and Physical Activity in People With Transtibial Amputation," Arch. Phys. Med. Rehabil., **87**(1), pp. 123–129.
[7] Burke, M. J., Roman, V., and Wright, V., 1978, "Bone and Joint Changes in Lower Limb Amputees," Ann. Rheum. Dis., **37**(3), pp. 252–254.
[8] Kulkarni, J., Gaine, W. J., Buckley, J. G., Rankine, J. J., and Adams, J., 2005, "Chronic Low Back Pain in Traumatic Lower Limb Amputees," Clin. Rehabil., **19**(1), pp. 81–86.
[9] Norvell, D. C., Czerniecki, J. M., Reiber, G. E., Maynard, C., Pecoraro, J. A., and Weiss, N. S., 2005, "The Prevalence of Knee Pain and Symptomatic Knee Osteoarthritis Among Veteran Traumatic Amputees and Nonamputees," Arch. Phys. Med. Rehabil., **86**(3), pp. 487–493.
[10] Neptune, R. R., Kautz, S. A., and Zajac, F. E., 2001, "Contributions of the Individual Ankle Plantar Flexors to Support, Forward Progression and Swing Initiation During Walking," J. Biomech., **34**(11), pp. 1387–1398.
[11] Zajac, F. E., Neptune, R. R., and Kautz, S. A., 2003, "Biomechanics and Muscle Coordination of Human Walking—Part II: Lessons From Dynamical Simulations and Clinical Implications," Gait Posture, **17**(1), pp. 1–17.
[12] Silverman, A. K., and Neptune, R. R., 2012, "Muscle and Prosthesis Contributions to Amputee Walking Mechanics: A Modeling Study," J. Biomech., **45**(13), pp. 2271–2278.
[13] Neptune, R. R., Sasaki, K., and Kautz, S. A., 2008, "The Effect of Walking Speed on Muscle Function and Mechanical Energetics," Gait Posture, **28**(1), pp. 135–143.
[14] Zmitrewicz, R. J., Neptune, R. R., and Sasaki, K., 2007, "Mechanical Energetic Contributions From Individual Muscles and Elastic Prosthetic Feet During Symmetric Unilateral Transtibial Amputee Walking: A Theoretical Study," J. Biomech., **40**(8), pp. 1824–1831.
[15] Au, S. K., Weber, J., and Herr, H. M., 2007, "Biomechanical Design of a Powered Ankle-Foot Prosthesis," IEEE Tenth International Conference on Rehabilitation Robotics (ICORR), Noordwijk, The Netherlands, June 13–15, pp. 298–303.
[16] Eilenberg, M. F., Geyer, H., and Herr, H. M., 2010, "Control of a Powered Ankle-Foot Prosthesis Based on a Neuromuscular Model," IEEE Trans. Neural Syst. Rehabil. Eng., **18**(2), pp. 164–173.
[17] Herr, H. M., and Grabowski, A. M., 2012, "Bionic Ankle-Foot Prosthesis Normalizes Walking Gait for Persons With Leg Amputation," Proc. Biol. Sci., **279**(1728), pp. 457–464.
[18] Ferris, A. E., Aldridge, J. M., Rábago, C. A., and Wilken, J. M., 2012, "Evaluation of a Powered Ankle-Foot Prosthetic System During Walking," Arch. Phys. Med. Rehabil., **93**(11), pp. 1911–1918.
[19] D'Andrea, S., Wilhelm, N., Silverman, A. K., and Grabowski, A. M., 2014, "Does Use of a Powered Ankle-Foot Prosthesis Restore Whole-Body Angular Momentum During Walking at Different Speeds?," Clin. Orthop. Relat. Res., **472**(10), pp. 3044–3054.
[20] Pickle, N. T., Wilken, J. M., Aldridge Whitehead, J. M., and Silverman, A. K., 2016, "Whole-Body Angular Momentum During Sloped Walking Using Passive and Powered Lower-Limb Prostheses," J. Biomech., **49**(14), pp. 3397–3406.
[21] Pickle, N. T., Wilken, J. M., Aldridge, J. M., Neptune, R. R., and Silverman, A. K., 2014, "Whole-Body Angular Momentum During Stair Walking Using Passive and Powered Lower-Limb Prostheses," J. Biomech., **47**(13), pp. 3380–3389.
[22] Gates, D. H., Aldridge, J. M., and Wilken, J. M., 2013, "Kinematic Comparison of Walking on Uneven Ground Using Powered and Unpowered Prostheses," Clin. Biomech., **28**(4), pp. 467–472.
[23] Lay, A. N., Hass, C. J., Nichols, T. R., and Gregor, R. J., 2007, "The Effects of Sloped Surfaces on Locomotion: An Electromyographic Analysis," J. Biomech., **40**(6), pp. 1276–1285.
[24] Lange, G. W., Hintermeister, R. A., Schlegel, T., Dillman, C. J., and Steadman, R., 1996, "Electromyographic and Kinematic Analysis of Graded Treadmill Walking and the Implications for Knee Rehabilitation.," J. Orthop. Sports Phys. Ther., **23**(5), pp. 294–301.
[25] Kuster, M., Sakurai, S., and Wood, G. A., 1995, "Kinematic and Kinetic Comparison of Downhill and Level Walking," Clin. Biomech., **10**(2), pp. 79–84.
[26] Pickle, N. T., Grabowski, A. M., Auyang, A. G., and Silverman, A. K., 2016, "The Functional Roles of Muscles During Sloped Walking," J. Biomech., **49**(14), pp. 3244–3251.
[27] Dorn, T. W., Wang, J. M., Hicks, J. L., and Delp, S. L., 2015, "Predictive Simulation Generates Human Adaptations During Loaded and Inclined Walking," PLoS One, **10**(4), p. e0121407.
[28] Alexander, N., and Schwameder, H., 2016, "Lower Limb Joint Forces During Walking on the Level and Slopes at Different Inclinations," Gait Posture, **45**, pp. 137–142.
[29] Alexander, N., and Schwameder, H., 2016, "Effect of Sloped Walking on Lower Limb Muscle Forces," Gait Posture, **47**, pp. 62–67.
[30] Walker, C. R. C., Ingram, R. R., Hullin, M. G., and McCreath, S. W., 1994, "Lower Limb Amputation Following Injury: A Survey of Long-Term Functional Outcome," Injury, **25**(6), pp. 387–392.
[31] Fey, N. P., Klute, G. K., and Neptune, R. R., 2013, "Altering Prosthetic Foot Stiffness Influences Foot and Muscle Function During Below-Knee Amputee Walking: A Modeling and Simulation Analysis.," J. Biomech., **46**(4), pp. 637–644.
[32] Fradet, L., Alimusaj, M., Braatz, F., and Wolf, S. I., 2010, "Biomechanical Analysis of Ramp Ambulation of Transtibial Amputees With an Adaptive Ankle Foot System," Gait Posture, **32**(2), pp. 191–198.
[33] Langlois, K., Villa, C., Bonnet, X., Lavaste, F., Fodé, P., Martinet, N., and Pillet, H., 2014, "Influence of Physical Capacities of Males With Transtibial Amputation on Gait Adjustments on Sloped Surfaces," J. Rehabil. Res. Dev., **51**(2), pp. 193–200.
[34] Wolf, S. I., Alimusaj, M., Fradet, L., Siegel, J., and Braatz, F., 2009, "Pressure Characteristics at the Stump/Socket Interface in Transtibial Amputees Using an Adaptive Prosthetic Foot," Clin. Biomech., **24**(10), pp. 860–865.
[35] Jeffers, J. R., Auyang, A. G., and Grabowski, A. M., 2015, "The Correlation Between Metabolic and Individual Leg Mechanical Power During Walking at Different Slopes and Velocities," J. Biomech., **48**(11), pp. 2919–2924.
[36] Lu, T. W., and O'Connor, J. J., 1999, "Bone Position Estimation From Skin Marker Co-Ordinates Using Global Optimisation With Joint Constraints," J. Biomech., **32**(2), pp. 129–134.
[37] Antonsson, E., and Mann, R., 1985, "The Frequency Content of Gait," J. Biomech., **18**(1), pp. 39–47.
[38] Kram, R., Griffin, T. M., Donelan, J. M., and Chang, Y. H., 1998, "Force Treadmill for Measuring Vertical and Horizontal Ground Reaction Forces," J. Appl. Physiol., **85**(2), pp. 764–769.
[39] Riley, P. O., Paolini, G., Della Croce, U., Paylo, K. W., and Kerrigan, D. C., 2007, "A Kinematic and Kinetic Comparison of Overground and Treadmill Walking in Healthy Subjects," Gait Posture, **26**(1), pp. 17–24.
[40] Kristianslund, E., Krosshaug, T., and van den Bogert, A. J., 2012, "Effect of Low Pass Filtering on Joint Moments From Inverse Dynamics: Implications for Injury Prevention," J. Biomech., **45**(4), pp. 666–671.
[41] Bisseling, R. W., and Hof, A. L., 2006, "Handling of Impact Forces in Inverse Dynamics," J. Biomech., **39**(13), pp. 2438–2444.
[42] Delp, S. L., Anderson, F. C., Arnold, A. S., Loan, P., Habib, A., John, C. T., Guendelman, E., and Thelen, D. G., 2007, "OpenSim: Open-Source Software to Create and Analyze Dynamic Simulations of Movement," IEEE Trans. Biomed. Eng., **54**(11), pp. 1940–1950.
[43] Delp, S., Loan, J., Hoy, M., Zajac, F., Topp, E., and Rosen, J., 1990, "An Interactive Graphics-Based Model of the Lower Extremity to Study Orthopaedic Surgical Procedures," IEEE Trans. Biomed. Eng., **37**(8), pp. 757–767.
[44] Anderson, F. C., and Pandy, M. G., 1999, "A Dynamic Optimization Solution for Vertical Jumping in Three Dimensions," Comput. Methods Biomech. Biomed. Eng., **2**(3), pp. 201–231.
[45] Zajac, F., 1989, "Muscle and Tendon: Properties, Models, Scaling, and Application to Biomechanics and Motor Control," Crit. Rev. Biomed. Eng., **17**(4), pp. 359–411.
[46] Davy, D. T., and Audu, M. L., 1987, "A Dynamic Optimization Technique for Predicting Muscle Forces in the Swing Phase of Gait," J. Biomech., **20**(2), pp. 187–201.
[47] Anderson, F. C., 1999, "A Dynamic Optimization Solution for a Complete Cycle of Normal Gait," Ph.D. dissertation, University of Texas at Austin, Austin, TX.
[48] Smith, J. D., Ferris, A. E., Heise, G. D., Hinrichs, R. N., and Martin, P. E., 2014, "Oscillation and Reaction Board Techniques for Estimating Inertial Properties of a Below-Knee Prosthesis," J. Visualized Exp., **87**, p. e50977.
[49] Fregly, B., and Zajac, F., 1996, "A State-Space Analysis of Mechanical Energy Generation, Absorption, and Transfer During Pedaling," J. Biomech., **29**(1), pp. 81–90.
[50] Hamner, S. R., Seth, A., and Delp, S. L., 2010, "Muscle Contributions to Propulsion and Support During Running," J. Biomech., **43**(14), pp. 2709–2716.
[51] Pinheiro, J., Bates, D., DebRoy, S., Sarkar, D., and R Development Core Team, 2013, "NLME: Linear and Nonlinear Mixed Effects Models—R package version 3.1-108," R Foundation for Statistical Computing, Vienna, Austria.
[52] Lenth, R., 2016, "Least-Squares Means: The R Package lsmeans," J. Stat. Software, **69**(1), pp. 1–33.
[53] Moirenfeld, I., Ayalon, M., Ben-Sira, D., and Isakov, E., 2000, "Isokinetic Strength and Endurance of the Knee Extensors and Flexors in Trans-Tibial Amputees," Prosthet. Orthot. Int., **24**(3), pp. 221–225.
[54] Isakov, E., Burger, H., Gregoric, M., and Marincek, C., 1996, "Isokinetic and Isometric Strength of the Thigh Muscles in Below-Knee Amputees," Clin. Biomech., **11**(4), pp. 233–235.
[55] Ackermann, M., and Van Den Bogert, A. J., 2010, "Predictive Simulation of Gait in Rehabilitation," Annual International Conference of the IEEE Engineering in Medicine and Biology Society (EMBC), Buenos Aires, Argentina, Aug. 31–Sept. 4, pp. 5444–5447.
[56] Wesseling, M., Derikx, L. C., de Groote, F., Bartels, W., Meyer, C., Verdonschot, N., and Jonkers, I., 2014, "Muscle Optimization Techniques Impact the Magnitude of Calculated Hip Joint Contact Forces," J. Orthop. Res., **33**(3), pp. 1–9.
[57] Myers, C. A., Laz, P. J., Shelburne, K. B., and Davidson, B. S., 2015, "A Probabilistic Approach to Quantify the Impact of Uncertainty Propagation in Musculoskeletal Simulations," Ann. Biomed. Eng., **43**(5), pp. 1098–1111.
[58] Dorn, T. W., Lin, Y., and Pandy, M. G., 2012, "Estimates of Muscle Function in Human Gait Depend on How Foot-Ground Contact is Modelled," Comput. Methods Biomech. Biomed. Eng., **15**(6), pp. 657–668.